Raman scattering in the ternary phase $HfS_{3-x}Se_x$

A. Zwick, G. Landa, M. A. Renucci, and R. Carles
Laboratoire de Physique des Solides associé au Centre National de la Recherche Scientifique, 118 Route de Narbonne, 31062 Toulouse Cédex, France

A. Kjekshus
Kjemisk Institutt, Universitetet i Oslo, Blindern, Oslo 3, Norway
(Received 11 May 1982)

The mode behavior of long-wavelength optical phonons in the ternary phase $HfS_{3-x}Se_x$ has been investigated by Raman spectroscopy through the whole composition range $0 \leq x \leq 3$. Previous studies on the parent compounds have shown that $\vec{k}=\vec{0}$ Raman-active modes can be classified according to largely rigid chain modes (group I), internal deformation chain modes (group II), and a stretching mode of the diatomic chalcogen X_2 pair within the chains (group III). A mixed one-, two-, and three-mode behavior is observed in the $HfS_{3-x}Se_x$ system, depending respectively on modes of group I, II, and III. This behavior reflects the quite different and specific atomic interactions governing these different groups. More precisely, the mode-number progression from group I to group III appears to be related to the corresponding shortening of the range of atomic interactions involved. In particular, three-mode behavior is observed for diatomic X_2 modes. This behavior results from vibrations of S-S, Se-Se, and S-Se pairs of chalcogen atoms covalently bound. The picture of diatomic X-X' (X,X'=S,Se) "molecules" is substantiated by an estimate of the S-Se mode frequency based on a molecular model, in good agreement with experimental data. In addition, we took advantage of one-mode behavior of group I to establish a one-to-one correspondence between compatible phonons in the pure end member crystals and thus resolve some discrepancies in mode assignment from different authors.

I. INTRODUCTION

The lattice-dynamical properties of compounds with the $ZrSe_3$-type structure have recently been given considerable attention. The chief aim of these efforts has been to provide a better understanding of the chemical bonding in these materials, which exhibit both chainlike and layerlike features. Long-wavelength optical-phonon modes have been investigated in the essentially isostructural compounds TiS_3,[1,2] ZrS_3, [3–7] $ZrSe_3$,[4,5,8] $ZrTe_3$,[2,6] HfS_3,[4,5,9] and $HfSe_3$ (Refs. 2 and 6) by means of infrared and Raman techniques. These studies have implied a major step forward in the overall charting of the bonding situation in the $ZrSe_3$-type structure. The time has now come for focusing the attention on spectroscopical and bonding details.

From a molecular model description[8] of the dynamical properties of the $ZrSe_3$-type structure it has proved possible to deduce valuable information about the relative strength of intrachain and interchain couplings. Lattice-dynamical calculations on the basis of valence force field models at $\vec{k}=\vec{0}$ by Grisel *et al.*[5] and Sourisseau and Mathey,[10] moreover, suggest that although the chains clearly are interlinked into layers, a distinct degree of one-dimensional character is still maintained. Unfortunately, the experimental data on $\vec{k}=\vec{0}$ optically active phonons are far from complete for these compounds. All 21 symmetry-predicted phonons have not yet been identified, and the literature demonstrates discrepancies between some of the studies. Consequently, there are ambiguities both in mode assignments for the individual compounds and in mode correspondence between the different compounds. These shortcomings suggest that it may be beneficial to examine the long-wavelength optical phonons in ternary phases of the $ZrSe_3$-type structure as a means to shed light on the properties of the parent compounds. Indeed, in the case of one-mode behavior in solid solution, a given mode

can, in principle, be followed continuously from one end member to the other. Moreover, as mode behavior in a solid solution must be related to the bonding properties, studies of ternary systems provide possibilities to test deductions and hypotheses advanced for the binary $ZrSe_3$-type compounds.

The present paper gives an account of Raman scattering experiments on the ternary phase $HfS_{3-x}Se_x$.

II. SYMMETRY CONSIDERATIONS ON THE $ZrSe_3$-TYPE CRYSTAL STRUCTURE

HfS_3 and $HfSe_3$ take the monoclinic $ZrSe_3$-type structure[11] (space group $P2_1/m$-C_{2h}^2). As outlined in Ref. 11, the $ZrSe_3$-type structure occurs in two different variants (related by a quasi-mirror-plane), but the effects of these structural details on the vibrational characteristics have not yet been examined. The $ZrSe_3$-type structure has both layerlike and chainlike features, *inter alia* responsible for a distinct fibrous appearance of the crystals and their easy cleavage along (001). According to the chain description, the $ZrSe_3$-type structure is built up of trigonal prisms of one metal and six chalcogens stacked on top of each other along the crystallographic [010]. The chains are further linked to form layers parallel to (001) by bicapping contacts between the prisms. The layers are, on the other hand, separated from the neighboring layers by distances which closely match the interatomic distances prescribed for van der Waals–type bonding. Figure 1(b) displays the primitive unit cell, with two chains and their interrelation, while a (010) projection of the $ZrSe_3$-type structure (variant I) is shown in Fig. 1(a).

Both crystal- and chain-factor group analyses of the long-wavelength phonon modes for the $ZrSe_3$-type structure are available from the literature.[4,8] The following decompositions are appropriate:

$$\Gamma_{\text{crystal}} = 8A_g + 4B_g + 4A_u + 8B_u \ ,$$

$$\Gamma_{\text{chain}} = 4A_1 + 4B_1 + A_2 + 3B_2 \ .$$

In contrast to the chain modes, the crystal modes divide into even- or odd-symmetry types with respect to the inversion, Raman and infrared active, respectively. Both crystal and chain modes can be classified according to the atomic displacements parallel (B_g and A_u for the crystal, A_2 and B_2 for the chain) or perpendicular (A_g and B_u, A_1 and B_1) to the chains.

The correlation diagram presented in Fig. 2

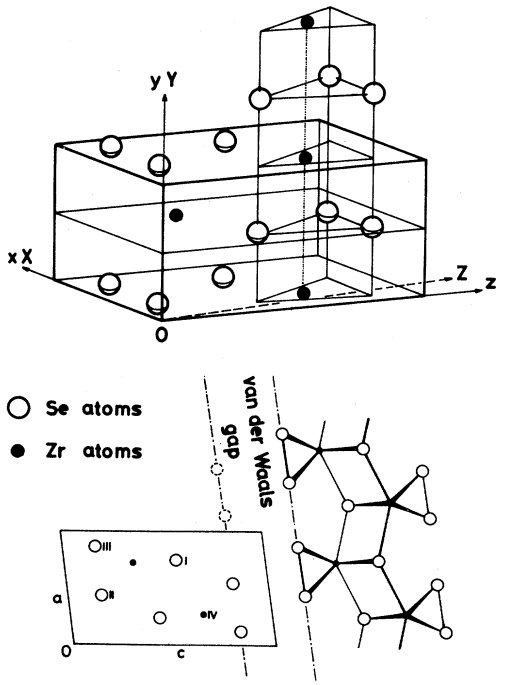

FIG. 1. $ZrSe_3$-type structure. (a) projection on (010); (b) two molecular units of the primitive cell. a,b,c and x,y,z denote crystallographic (second setting) and principal axes, respectively.

shows the compatibility relationship between the chain and crystal modes and illustrates how crystal modes are generated from single-chain modes as the interchain coupling is included in the con-

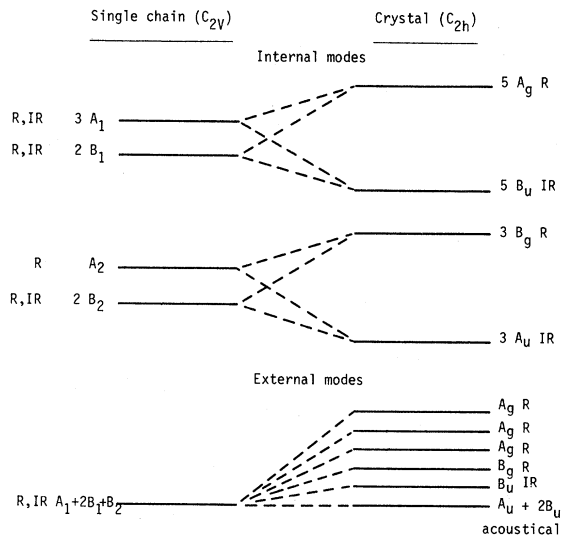

FIG. 2. Correlation diagram relating the $\vec{k}=\vec{0}$ chain and crystal modes of the $ZrSe_3$-type structure (R = Raman, IR = infrared).

siderations. The following features are notable:

(i) Each chain mode splits into a *g-u* pair of crystal modes. This originates from the fact that the two chains of the primitive unit cell are connected via an inversion center.

(ii) The chain modes A and B become mixed-crystal modes. The reason for this is that the crystal symmetry does not allow the twofold axis of the chain description.

(iii) The four low-frequency Raman crystal modes $3A_g+B_g$ derived from the essentially zero-frequency modes of the chain description $A_1+2B_1+B_2$ reflect largely rigid-chain motions, viz., three translational modes along the axes a, b, and c (A_g,B_g,A_g) and one librational mode about the b axis (A_g).

III. RAMAN SPECTRA FOR HfS_3 AND $HfSe_3$

The long-wavelength optical-phonon modes in HfS_3 (Refs. 4, 5, and 9) and $HfSe_3$ (Refs. 2 and 6) have recently been investigated by means of infrared and Raman spectroscopy. Too few of the theoretically predicted $\vec{k}=\vec{0}$ Raman- and/or infrared active modes have been observed for the two compounds to render mode assignment reasonably unambiguous. As a background for our analyses of the Raman modes of the solid-solution phase $HfS_{3-x}Se_x$, Table I summarizes all available Raman data from the literature for the parent compounds HfS_3 and $HfSe_3$. Table I also includes fresh data for HfS_3 derived from analyses of the polarized Raman spectra displayed in Fig. 3.

A few brief comments on Table I appear appropriate. As was pointed out in Sec. II, the three lowest-lying modes of A_g symmetry are expected to be of largely rigid-chain character. Consequently, it is tempting to interpret the three A_g lines at 74, 111, and 130 cm^{-1} in HfS_3 in accordance with this, and correlate them with corresponding (rigid-chain) lines at 51, 69.5, and 101 cm^{-1} in $HfSe_3$. This interpretation excludes the A_g line reported by Wieting *et al.*[4] at 15 cm^{-1} in HfS_3 as a possible rigid-chain mode, although we thus have no explanation to offer for the appearance of a weak structure at this frequency also in the present spectra. Our polarization experiments (see Fig. 3) confirm the assignment of A_g symmetry to the 130-cm^{-1} line in HfS_3 as proposed by Wieting *et al.*[4] This finding implies that we disagree with the interpretation of Deville-Cavellin and Jandl,[9] which we moreover consider as inconsistent with the spectral data published by the latter authors. Furthermore, the present results clearly establish B_g symmetry for the modes located at 218 and 246 cm^{-1}, and which previously have only been recorded by Deville-Cavellin and Jandl.[9] Their counterparts in $HfSe_3$ appear, on the other hand, to be missing. We have failed to identify the rather broad structure at 275 cm^{-1}, previously reported by Grisel[12] and Deville-Cavellin and Jandl.[9]

TABLE I. Observed wave numbers and symmetries for $\vec{k}=\vec{0}$ Raman modes in HfS_3 and $HfSe_3$ at 300 K.

HfS_3						$HfSe_3$					
Refs 4 and 5		Ref. 9		Our work		Ref. 2		Ref. 6		Group of lines	Modes of isolated chains
Symmetry	ν (cm^{-1})	Symmetry	ν (cm^{-1})	Symmetry	ν (cm^{-1})	Symmetry	ν (cm^{-1})	Symmetry	ν (cm^{-1})		
A_g	15			A_g	(17)	A_g	19				
A_g	73			A_g	74	A_g	69	A_g	51		
				A_g	111			A_g	69.5	I	Rigid
A_g	127	B_g	130	A_g	130	A_g	101	A_g	101		
B_g	140	B_g	140	B_g	140.5	B_g	69	B_g	69		
		B_g	221	B_g	218						
		B_g	246	B_g	246						
A_g	261	A_g	262	A_g	260	A_g	171	A_g	171		
				A_g	264			A_g	171.5	II	Internal
		A_g	275	A_g	275						
A_g	322	A_g	322	A_g	322	A_g	209	A_g	209		
				A_g	340						
A_g	524	A_g	527	A_g	525.5	A_g	296	A_g	295	III	Diatomic X-X

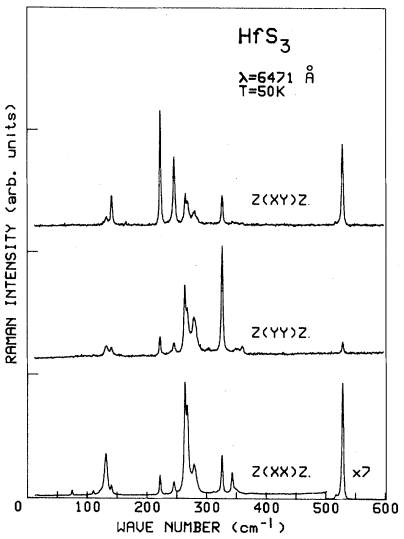

FIG. 3. Polarized Raman spectra of HfS_3 excited with $\lambda = 6471$ Å at 50 K. Notation for different configurations stands for $\vec{k}_i(\vec{e}_i,\vec{e}_s)\vec{k}_s$, where $(\vec{k}_i,\vec{e}_i)$ and $(\vec{k}_s,\vec{e}_s)$ are, respectively, wave vector and polarization vector of incident and scattered light.

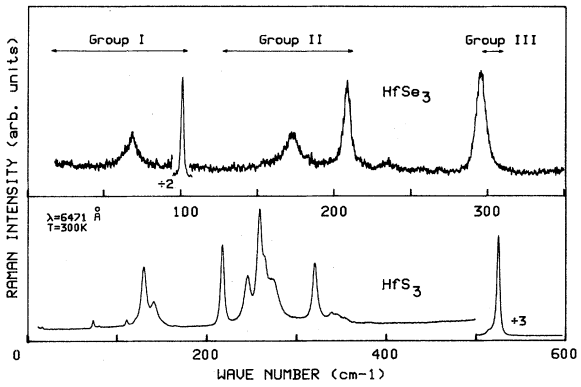

FIG. 4. Unpolarized Raman spectra of (a) HfS_3 and (b) $HfSe_3$ excited with $\lambda = 6471$ Å at room temperature. For the notations of groups I–III, see text.

As references for our powder Raman study of the $HfS_{3-x}Se_x$ solid solution phase, we present in Fig. 4 unpolarized spectra from single crystals of HfS_3 and $HfSe_3$. These spectra are quite similar, with well-separated groups of lines. In the order of increasing frequency, we observe:

(i) A first group (I) in the low-frequency region, originating from rigid-chain modes which in the limiting case may be regarded to have zero coupling between adjacent chains.

(ii) A second group (II), which in terms of the same limitation as in (i) corresponds to internal deformations of the chains.

(iii) A single line (III) separated from the others by a large gap in energy, attributed to the stretching of the $X_{II} - X_{III}$ pair bond (X = S,Se; indices I–III refer to crystallographic different atoms of the $ZrSe_3$-type structure[11]).

IV. RAMAN DATA FOR $HfS_{3-x}Se_x$

The present $HfS_{3-x}Se_x$ samples were polycrystalline powders prepared as described by Brattås and Kjekshus,[13] regularly spaced in the concentration range with $x = 0.5, 1.0, 1.5, 2.5$. The homogeneity of the samples were ascertained from powder x-ray (Guinier) photographs.

Raman spectra were taken at room and low (when improved resolution was necessary) temperature. A helium atmosphere was used to avoid combustion of the powder samples as well as to remove scattering from the air. The Raman spectra were excited with the 6471-Å line of a Kr^+ laser, selected in order to minimize absorption and resonance effects. A suitable scattering geometry was chosen to eliminate most of the unwanted elastic scattering from irregularities. The Raman signals were analyzed by a T800 CODERG triple monochromator in combination with photon counting electronics.

The 300-K Stokes spectra of $HfS_{3-x}Se_x$ are presented in Fig. 5 together with those of single crystals of HfS_3 and $HfSe_3$ for comparison. The Raman spectrum of $HfS_{2.5}Se_{0.5}$ may be taken as a typical example. This shows features derived from both end members in addition to a new line originating from the mixed system. The identifiable peaks, which are numbered 1 to 11 on this spectrum, all originate from A_g modes in the binary compounds. Corresponding lines in the various spectra in Fig. 5 are seen to vary appreciably in intensity, but scarcely in peak position.

An additional structure appears near 235 cm^{-1} in all samples containing Se, i.e., $HfS_{2.5}Se_{0.5}$ to $HfSe_3$, the frequency being independent of composition. This structure corresponds to the A_1 mode of trigonal selenium and was already observed for nonfreshly cleaved single crystals of $HfSe_3$.[6] The Se is likely to result from surface oxidation which leaves Se behind.

No additional information could be derived from

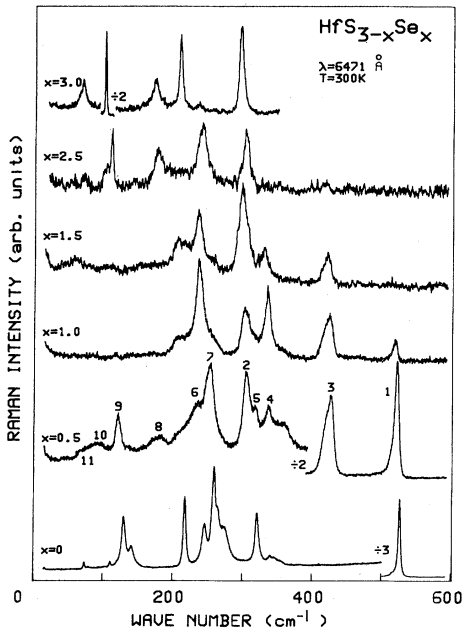

FIG. 5. Unpolarized Raman spectra of $HfS_{3-x}Se_x$ excited with $\lambda = 6471$ Å at room temperature. For numbering of the lines on the $HfS_{2.5}Se_{0.5}$ spectrum, see text.

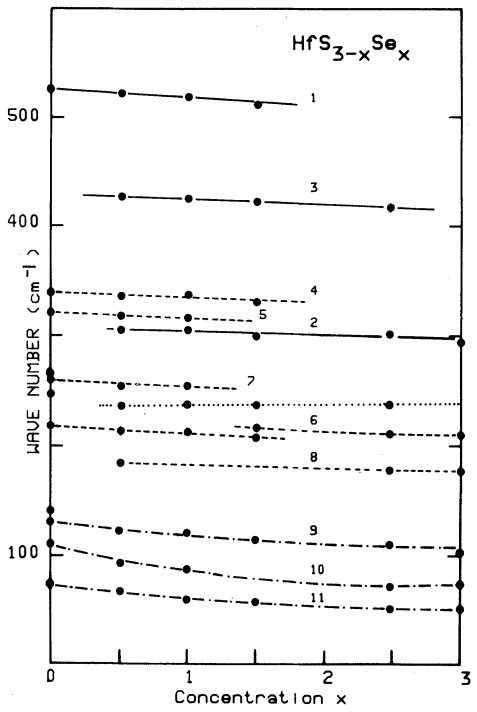

FIG. 6. Mode wave numbers of $HfS_{3-x}Se_x$ as function of compositional parameter x.

the low-temperature spectra as there is a considerable decrease in intensity, particularly for the low-frequency lines, which makes the detection of signals below 150 cm^{-1} very difficult.

Figure 6 gives the frequency of the identifiable peaks as a function of the compositional parameter x. $HfS_{3-x}Se_x$ appears to be an interesting solid-solution system that displays a mixed one-, two-, and three-mode behavior, depending on the long-wavelength optical modes. The Raman lines of the system can be classified according to the group from which they originate in the binary compounds (cf. Sec. III).

A. Modes of group III

1. Line 1 (525.5—512 cm^{-1})

At the HfS_3 end, this line starts from the A_g peak corresponding to the S-S—pair stretching mode. For increasing concentration of Se, there is a slight shift in frequency and a decrease in intensity. The line is not detectable for $x > 1.5$.

2. Line 2 (305—295 cm^{-1})

This line is not found in HfS_3, but appears for $x = 0.5$. Its frequency decreases with increasing Se content and attains the value corresponding to the Se-Se—pair mode at the $HfSe_3$ end.

3. Line 3 (426—417 cm^{-1})

Besides the lines already described, reminiscent from S-S and Se-Se stretching modes of the binary end member crystals, a third mode appears in the solid solution over the whole range of concentration, and at a frequency midway between those of the S-S—and Se-Se—like modes. The temperature dependence of this line excludes that it originates from a second-order scattering process. The observed linewidth and frequency (see the discussion on the dispersion curves) also rule out assignment to some disorder-activated zone-edge phonon. This leads to the inference that this line corresponds to a new long-wavelength optical mode of the mixed system.

The conclusion is accordingly that the stretching mode of the X-X pair of the $ZrSe_3$-type structure exhibits a three-mode behavior.

B. Modes of group II

1. Line 4 (340—332 cm^{-1})

This line starts from the A_g peak at 340 cm^{-1} in HfS_3, and shifts towards slightly lower frequencies with increasing Se content. Its intensity seems surprisingly related to that of the structure at 235 cm^{-1}, which we already have attributed to trigonal selenium. As there is no compatible partner to this mode in neither Se nor $HfSe_3$, further speculations seem unprofitable.

2. Sets of lines 5 and 6 (322—315 cm^{-1} and 212—209 cm^{-1}) and of lines 7 and 8 (260—252 cm^{-1} and 180—173.5 cm^{-1})

Each set occurs at frequencies close to those of the strongest A_g modes of group II in the binary end member crystals, observed at 322 and 260 cm^{-1} in HfS_3, 209 and 173.5 cm^{-1} in $HfSe_3$, respectively. The intensity of a given of these phonon lines increases with increasing content of the appropriate component (S or Se). These features are characteristic of two-mode behavior.

C. Modes of group I

As previously mentioned, a certain unavoidable amount of stray light admixes to the weak intensity of the low-frequency peaks even for the binary compound crystals. This makes the detection of signals very difficult below 150 cm^{-1}. Nevertheless, the A_g mode of HfS_3 at 130 cm^{-1} (line 9) is seen to evolve continuously throughout the composition range, terminating at the A_g mode of $HfSe_3$ at 101 cm^{-1}. The two other low-frequency A_g modes (lines 10 and 11) seem to behave in the same manner although it was impossible to follow them through the whole composition interval.

Modes originating from rigid-chain modes of the parent crystals therefore appear to follow a one-mode behavior in the mixed system.

V. DISCUSSION OF MODE BEHAVIOR

Essentially two types of solid-solution systems can be distinguished with respect to the long-wavelength optical phonons versus composition behavior.[14] In the "one-mode" case, each of the $\vec{k}=\vec{0}$ optical-mode frequencies varies continuously with concentration, from the frequency characteristic of the one end member to that of the other. In the "two-mode" case, two sets of $\vec{k}=\vec{0}$ optical modes occur at frequencies close to those of the end members. Most of the alkali-metal halide solid-solution phases exhibit "one-mode" behavior, whereas the "two-mode" behavior is commonly observed for the III-V and II-VI compound solid-solution phases.

A less common type of multimode behavior has been reported in element solid-solution systems like $Ge_{1-x}Si_x$,[15] $Te_{1-x}Se_x$,[16] and $Bi_{1-x}Sb_x$,[17] where an additional mode results from bonds between the unlike atoms.

The models advanced[14] hitherto for prediction of the mode versus composition behavior for solid-solution phases are limited to simple lattice structures (cubic symmetry with two atoms per unit cell). Consequently, it is hardly to be expected that these simple models should be able to cope with the rather complicated and anisotropic $ZrSe_3$-type structure. A model based solely on the masses of the constituent atoms cannot, in principle, predict the coexistence of one-, two-, and three-mode behavior in the $HfS_{3-x}Se_x$ system.

According to the theory of localized modes,[14] one may raise the question of local versus gap modes near the ends of the solid-solution range. Testing of the predictions of the theory requires data for phonon bands in the binary compounds.

Although the phonon dispersion curves of HfS_3 and $HfSe_3$ are unknown, we may from zone-center modes deduce some general trends about the phonon bands in the binary compounds. Indeed, the frequency range covered by the group I, II, and III, $\vec{k}=\vec{0}$ modes in HfS_3 and $HfSe_3$ (Fig. 6) allows an estimate for the corresponding phonon bands.

The acoustical and the first optical bands of HfS_3 and $HfSe_3$, originating from acoustical chain modes, are expected to be considerably overlapped. They may effectively cover broader regions in the frequency space than the optical zone-center modes of group I (already overlapping to a large extent). This assumption rules out the possibility of local modes of Se in HfS_3 and of S in $HfSe_3$ in the lowest-frequency range, and excludes a general multimode behavior of the modes of group I. The third optical bands originating from the molecular-like S-S— and Se-Se—pair modes should be practically $\vec{k}$ independent, and thus separated by a large energy gap, a situation which favors the multimode behavior of group III. Within the same framework, no conclusion can be drawn for the mode

behavior of the group-II modes. The case here is that we cannot exclude the possibility of overlap for corresponding optical branches of the end member crystals.

At this point it may be pertinent to emphasize the close relationship between mode behavior and bonding. Multiple-mode behavior has only been observed in solid solutions of simple structures where nearest-neighbor interaction dominates, such as the binary phases of the group-IV, -V, and -VI elements or ternary phases of the III-V or II-VI compounds. The three-mode behavior of $Ge_{1-x}Si_x$, Bi_{1-x} Sb_x, $Se_{1-x}Te_x$, the two-mode behavior of $GaAs_{1-x}P_x$, etc., are believed to reflect particular types of local interatomic configurations. On the other hand, one-mode behavior prevails in mixed crystals where long-range forces are predominant. In the latter situation a given atom in the mixture feels forces originating from far beyond its local environment. As evident from the above, one-mode behavior is frequently encountered in alkali-metal halide solid solutions, where the long-range forces are of an electromagnetic nature.

The various one-, two-, and three-mode behavior of the $HfS_{3-x}Se_x$ system may therefore reflect the quite different and specific interatomic interactions governing the particular mode. From the observed mode behavior, it is tempting to suggest that longer- and longer-range interactions become involved when going from group-III to group-I modes. This suggestion is consistent with the lattice-dynamical calculations (on the basis of valence force-field models) at $\vec{k}=\vec{0}$ by Wieting *et al.*[2] and Sourisseau and Mathey.[7] These calculations demonstrate *inter alia* that:

(i) The *X*-*X* mode of group III depends mainly on the nearest-neighbor interaction between the pairing chalcogen (*X*) atoms in the chains.

(ii) Modes of group II are largely governed by metal-chalcogen interactions within the chains.

(iii) Modes of group I involve longer-range interactions between atoms of adjacent chains.

The three-mode behavior of group III which appears to result from vibrations of the S-S, Se-Se, and S-Se pairs confirms the covalent nature of the bonding within the *X*-*X* pairs. Jellinek *et al.*[18] have arrived at the same conclusion by x-ray photoemission measurements. An estimate of the third S-Se—mode frequency can be obtained from the diatomic frequencies of HfS_3 and $HfSe_3$, and this provides a further support for the *X*-*X* "molecular" picture. Angular frequencies of diatomic modes are effectively given by

$$\omega^2_{X\text{-}X'}=k_{X\text{-}X'}\left[\frac{1}{m_X}+\frac{1}{m_{X'}}\right], \quad X,X'=\text{S, Se},$$

where $m_{X\,(X')}$ is the mass of X (X') and $k_{X\text{-}X'}$ the force constant assigned to the central X-X' interaction in the nonsymmetric "molecule." As the diatomic modes in HfS_3 and $HfSe_3$ approximately scale with the atomic masses of X (X'), we choose for $K_{S\text{-}Se}$ the average of $k_{S\text{-}S}$ and $k_{Se\text{-}Se}$. The introduction of

$$\omega^2_{S\text{-}Se}=\frac{k}{\mu},$$

where $\mu^{-1}=m_S^{-1}+m_{Se}^{-1}$ gives

$$\omega^2_{S\text{-}Se}=\tfrac{1}{2}(\omega^2_{S\text{-}S}+\omega^2_{Se\text{-}Se}).$$

With $\nu_{S\text{-}S}=525.5$ cm^{-1} and $\nu_{Se\text{-}Se}=295$ cm^{-1}, this relation gives a wave number of 426 cm^{-1}, in rather good agreement with the experimental data.

In a recent paper, Jandl[19] reports a peak at 426 cm^{-1} in $ZrS_{2.5}Se_{0.5}$ which he, however, attributes to a local mode. The *X*-*X*—pair modes of Zr and Hf trichalcogenides are rather insensitive to the metal atoms ($\nu_{S\text{-}S}=529$ and 525.5 cm^{-1} in ZrS_3 and HfS_3, respectively; $\nu_{Se\text{-}Se}=302$ and 295 cm^{-1} in $ZrSe_3$ and $HfSe_3$, respectively). Hence, we expect the line associated with the vibration of the S-Se pairs to occur practically at the same frequency in the $ZrS_{3-x}Se_x$ and $HfS_{3-x}Se_x$ systems. Our assignment is therefore consistent with the experimental data of Jandl.

VI. DEDUCTIONS AND NEW QUESTIONS

Despite the poor Raman efficiency of the low-frequency modes of $HfS_{3-x}Se_x$, the one-mode behavior of line 9 is unequivocally established over the whole composition range. Consequently, the continuous shift of this A_g-mode line from 130 cm^{-1} in HfS_3 to 101 cm^{-1} in $HfSe_3$ confirms that they are corresponding partners in the binary compounds, in accordance with previous assignments (see Table I).

The approximately linear relationship between the S-S—, S-Se—, and Se-Se—mode wave number and the compositional parameter x may be extended as a means to estimate the wave numbers of impurity modes that arise on the substitution of the chalcogen atoms. ($x=0.5$ and 2.5 correspond to $\sim$17 at.% of S and Se, respectively.) Extrapolation in Fig. 5 of the S-S and S-Se wave numbers for $x\rightarrow 3$ yields the wave numbers of local modes of S

in $HfSe_3$, ν_{l_1} ($HfSeSe_2$:S_2) = 502 cm^{-1} and ν_{l_2} ($HfSeSe_2$:S) = 414 cm^{-1} at room temperature. The corresponding wave numbers for the gap modes of Se in HfS_3, ν_{g_1} ($HfSS_2$:Se_2) = 307 cm^{-1} and ν_{g_2} ($HfSSe_2$:Se) = 428 cm^{-1}, are similarly obtained from the extrapolation of the Se-Se and S-Se wave numbers for $x \to 0$.

The peak attributed to the S-Se—pair mode actually develops an asymmetric tail on the low-frequency side. At low temperature, this peak is resolved into a doublet for the S-rich samples. The splitting of the two peak components decreases with decreasing sulfur content, as illustrated in Fig. 7, which displays the S-Se and S-S peaks at 77 K. The asymmetric lineshape is evident for both peaks. In particular the weak structure on the low-frequency side of the peak in pure HfS_3 should be denoted. A similar observation has also been made for ZrS_3 by Sourisseau and Mathey,[10] who attributed the phenomenon to an isotopic effect. An isotopic effect involving vibrations of ^{34}S-Se and ^{32}S-Se pairs could explain the occurrence of the doublet and gives the right order for the splitting. Indeed, the isotope splitting should be:

$$\frac{\Delta\nu_{\text{S-Se}}}{\nu_{\text{S-Se}}} = -\frac{1}{2}\frac{\mu}{m_{\text{S}}}\frac{\Delta m_{\text{S}}}{m_{\text{S}}},$$

which gives $\Delta\nu_{\text{S-Se}} = 9$ cm^{-1}, in good agreement with the observed $\Delta\nu_{\text{S-Se}} \sim 8$ cm^{-1}. Nevertheless, this explanation is far from satisfactory. The relative intensity of the two components of the doublet does not correspond to the relative natural abundance of the isotopes ^{32}S and ^{34}S ($\sim$96% and $\sim$4%, respectively). Furthermore, a similar isotopic effect should also be observed for selenium in $HfSe_3$. Hence, the occurrence of this fine structure in the $HfS_{3-x}Se_x$ spectra is clearly open for further experimental and/or theoretical considerations.

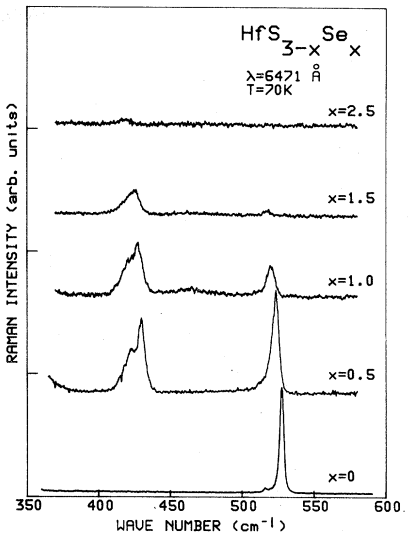

FIG. 7. Line shapes of S-Se and S-S peaks at 77 K ($0 \leq x \leq 2.5$).

[1]D. W. Galliardt, W. R. Nieveen, and R. D. Kirby, Solid State Commun. 34, 37 (1980).
[2]T. J. Wieting, A. Grisel, and F. Lévy, Physica B 105, 366 (1981).
[3]J. Y. Harbec, C. Deville-Cavellin, and S. Sandl, Phys. Status Solidi B 96, K117 (1980).
[4]T. J. Wieting, A. Grisel, F. Lévy, and Ph. Schmid, in *Proceedings of the International Conference on Quasi One Dimensional Conductors, Dubrovnik,* edited by S. Barisich (Springer, Berlin, 1979), p. 354.
[5]A. Grisel, F. Lévy and T. J. Wieting, Physica B 99, 365 (1980).
[6]A. Zwick, M. A. Renucci, and A. Kjekshus, J. Phys. C 13, 5603 (1980).
[7]C. Sourisseau and Y. Mathey, Chem. Phys. 74, 128 (1980).
[8]A. Zwick and M. A. Renucci, Phys. Status Solidi B 96, 757 (1979).
[9]C. Deville-Cavellin and S. Jandl, Solid State Commun. 33, 813 (1980).
[10]C. Sourisseau and Y. Mathey, Chem. Phys. 63, 143 (1981).
[11]S. Furuseth, L. Brattås, and A. Kjekshus, Acta Chem. Scand. Ser. A 29, 623 (1975).
[12]A. Grisel, Ph.D. thesis, Ecole Polytechnique Fédérale, Lausanne, 1981 (unpublished).
[13]L. Brattås and A. Kjekshus, Acta Chem. Scand. 26, 3441 (1972).
[14]I. F. Chang and S. S. Mitra, Adv. Phys. 20, 259 (1971).
[15]M. A. Renucci, J. B. Renucci, and M. Cardona, in *Proceedings of the Second International Conference on Light Scattering in Solids,* edited by M. Balkanski (Flammarion, Paris, 1971), p. 326.
[16]Geick, E. F. Steigmeier, and H. Auderset, Phys. Status Solidi 54, 623 (1972).
[17]R. N. Zitter and P. C. Watson, Phys. Rev. B 10, 607 (1974).
[18]F. Jellinek, R. A. Pollak, and M. W. Shafer, Mater. Res. Bull. 9, 845 (1974).
[19]S. Jandl and R. Provencher, J. Phys. C. 14, L461 (1981).